Aerotecnica Missili & Spazio, *The Journal of Aerospace Science, Technology and Systems*

Multi-objective Optimization for the Design of an Unconventional Sun-Powered High-Altitude-Long-Endurance Unmanned Vehicle

F. Mastroddi[a], L.M. Travaglini[a], S. Gemma[b]

[a] "Sapienza" - Università di Roma
Dipartimento di Ingegneria Meccanica e Aerospaziale

[b]Thales Italian Space

Abstract

The use of High Altitude and Long Endurance (HALE) Unmanned Aerial Vehicles (UAVs) is becoming increasingly significant in both military and civil missions as High-Altitude Pseudo-Satellite (HAPS). Since this class of aircraft is usually powered by solar cells, it typically features unconventional configurations to maximize sun exposed surfaces. In the present paper, a Multidisciplinary Design Optimization (MDO) and a Multi-Objective Optimization (MOO) environment have been developed to provide a computational design tool for modeling and designing these unconventional aircraft in order to achieve as independent objectives the maximization of solar power flux, the maximization of the lift-to-drag ratio, and the minimization of mass. To this purpose, a FEM models generator, capable of managing unconventional geometries, and a solar power estimator, are suitably developed to be integrated within a multi objective optimization loop. The simultaneous use of MDO/MOO approaches, and Design Of Experiment (DOE) creation and updating principles, enables to efficiently take into account the multiple and contrasting objectives/constraints arising from the different disciplines involved in the design problem. The study is carried out by using two different commercial codes for multi-objective optimization and for structural and aeroelastic analyses respectively. The use of advanced MDO/MOO approaches revealed to be effective for designing unconventional vehicles.

Acronyms and Symbols

- DOE: Design Of Experiment
- FEM: Finite Element Method
- HALE: High Altitude Long Endurance
- HAPS: High Altitude Pseudo Satellite
- LCU: Left of the Closest to Utopia point
- MDO: Multidisciplinary Design Optimization
- MOGA: Multi-Objective Genetic Algorithm
- MOO: Multi-Objective Optimization
- RCU: Right of the Closest to Utopia point
- RPAS: Remotely Piloted Aerial System
- SOO: Single-Objective Optimization
- UAV: Unmanned Aerial Vehicle
- ϕ: Energy flow
- E: Lift-to-Drag ratio
- L: Lift
- C_L: Lift coefficient
- D: Drag
- C_D: Drag coefficient
- W: Mass Weight
- e: Oswald efficiency number
- $\vec{v}_{sun}$: Sun rays energy vector
- $\vec{n}_i$: Normal to the i-th panel surface area
- S_i: i-th panel surface area

1. Introduction

HALEs are particular UAVs that make long time of flying aloft and high cruise altitudes in a range of 10-23 kilometers as their principal characteristics. This new perspective of application might change scenarios of Earth observation and surveillance. Indeed, HALEs most relevant applications are surveillance and Earth observing, since they have the capability of carrying out most of the tasks performed by standard LEO (Low Earth Orbit) satellites with consequent strong

reduction of the costs. For this reason, some of these UAVs that are equipped for Earth observation are also denoted as High-Altitude Pseudo-Satellite (HAPS). Moreover, HALEs can be also powered with green energy sources as solar panels (as Zephyr by AIRBUS Defence and Space, Ref. [1]). Solar panels may be used for this configuration for the following three principal motivations: providing the necessary energy to the propulsion system (often by means of brush-less propeller engines); charging the batteries (as the power supply for the night flying aloft); satisfying the energy need for the avionic instruments and payload, as the power system of such a platform consists of the three main subsystems, Ref. [2], [29]: *i)* power source; *ii)* energy storage; *iii)* electrical propulsion system. The HALE studied in the present work has been thought flying at Equatorial latitudes during summer season. This is the best condition for the solar panels and it has been chosen in order to simplify the studied model.

HALE UAV's typically have light and flexible structures. Lightness need has induced to the massive use of composite materials. Hybrid solutions for materials have been also proposed with an inner Aluminum skeleton, that acts as a support for the carbon skin, and solar panels. Unconventional shapes (Ref. [31]) seems to be important to face off the challenging requirements of the mission to which HALE will be assigned to. The most advanced prototypes that have been (till now) produced are Zephyr by AIRBUS Defence and Space, Ref. [1], Helios by Nasa, Ref. [3], Aquila By Facebook, Ref. [4], and, including also manned solution, Solar Impulse, Ref. [5]. Solar Challenger, Pathfinder and Global Observer, Sunseeker and Icar II enrich the scenario of solar powered aircraft. All of these solutions are actual examples of efforts that have been performed in order to find design compromises between lightness and structural strength, energy consumption reduction, especially in wintertime (Ref. [31]), and high performances. Moreover, Helios by Nasa crash focus the attention on all the problems that this type of structure design has to face off (Ref. [30]). future capabilities of HALEs platforms, Ref. [5].

The HALE studied in the present work -namely a HAPS- is an unmanned vehicle that has been thought for two different missions like ground observation (photogrammetry) and surveillance. The HALE could fly aloft, with almost circular trajectory, on a moving or fixed target, that must be monitored and chased. The strongest advantages with respect to a satellite are not only connected to the mission costs. For example, if necessary, a HALE could be fully operative in a few hours, with simple maneuvering capabilities.

The characteristics of the studied UAV are summarized in the following: *i)* very low weight; *ii)* adequate structural strength; *iii)* high lift-to-drag ratio. An aircraft with a high L/D ratio can carry a large payload, for a long time, over a long distance; *iv)* high capability of energy generation and storage, that means a high solar panel coverable surface and the possibility of carrying batteries.

About the structural strength, it is important to point out that HALEs design may induce to go beyond the standard structure of a conventional aircraft, Ref. [1]. The idea of spars and stringers is overcome by the concept of a light inner structure able to uniformly distribute loads. The skins have the only aim of transferring the aerodynamic loads to the skeleton. The use of a lattice structure helps in weight reduction in comparison to a conventional wing structure, for example, through the absence of steel spars. Full composites structures or hybrid Aluminum-composites structure are often used (see Ref. [6]. In the present paper, the hybrid solution has been chosen (Aluminum skeleton and carbon skin), in order to test the different material handling capability of the used tool.

From an energy efficiency point of view, the batteries are necessary in order to store energy that could be used during day time with low level or absence of sun light. This means that during the day the sun captured energy has to be maximized. This aim could be reached following two different approaches: *i)* increasing the exposed surface, so the weight as well or, *ii)* optimizing the aircraft and its mission in order to have, during all the day, the higher portion of wing surface as perpendicular as possible to sun rays.

All these considerations are addressed toward the choice of a closed-wing configuration. Indeed, the reasons justifying this choice are of aerodynamic and structural nature. More specifically:

- The box wing configuration, also know as Prandtl's Best Wing System (Ref. [7]), is able to minimize the lift induced drag and realizes the following conditions: identical lift distribution on upper and lower horizontal wings and linear distribution on the vertical wings. This configuration is demonstrated to be optimal with respect to wings having the same aspect ratio and the vortex induced velocities are constant on the wings and null on both the vertical sections, Ref. [8];

- The closed wing configuration is hyper-static. Thus, the global stiffness is heavily reinforced by the shape itself;

- The possibility of having, during all the day, parts of the surface enlightened by the sun, from midday to the sunset, where the vertical box-wing sections show all their relevance.

Although the closed wing configuration seems to be a convenient choice, in order to have the best advantages from it, a Multidisciplinary Design Optimization ap-

proach has been addressed. The MDO is a design technique that, in the last years, has taken every day more and more relevance in aeronautical design, Ref. [9]. In the advanced aerostructural design, MDO could be the most powerful ally in the next future, Refs. [10] and [11]. However, a lot of industries keep to be still linked to traditional design methods, basing the design of new products on their previous state of art. In the present work, a genetic algorithm, combined with a gradient based one, has been selected for carrying out the computation.

Thus, starting by the preliminary initial design presented in Fig. 1, three different objectives have been chosen for MOO analysis as a consequence of the missions requirements:

- Maximum lift to drag ratio;
- Maximum caught Sun power;
- Minimum weight.

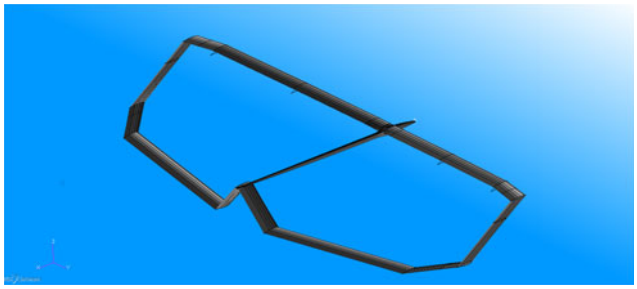

Figure 1. Proposed HALE 3D rendering.

Purpose of the present work, is not to study and optimize the overall mission of the introduced HALE configuration from takeoff to landing, but to assess the capability of multi-disciplinary and multi-objective approaches for optimizing a single mission phase. This is carried out through analyzing a specific segment of the flight, namely, when the HALE is on target. Note also that this optimization strategy is not addressed to optimize the amount of power needed, but only to maximize the lift-to-drag ratio as general parameter representative of this performance index. In order to focus the scope of the work, some assumptions about the mission are presented in Table 1. Therefore, focusing on the loitering phase only, it was relevant to develop a computational environment capable of including the solar energy flow in the optimization process. The analysis on the loitering phase is, of course, limited in the framework of the global mission, a starting point for further development that will take into account, for example, take-off and landing phases, ascent of the aircraft (typically spiral trajectory), and so on.

Table 1
Mission assumptions.

Object	**Assumption**
Latitude Angle	Equatorial trajectory
Day of the year	Summer solstice
Loiter altitude	20000 m, $\rho = 0,089 Kg/m^3$
Payload mass	$1.25 Kg$ Phase One iXU150
Payload Power Demand	$10 W$ Phase One iXU150

About the referred technologies in the present preliminary design, the set of used parameters are presented in Table 2 (see Ref. [28]). HALE propulsion system is assumed to be composed by two engines per half-wing (see Fig. 2). Batteries pack is located along fuselage symmetry axes with a total mass about a quarter than overall model weight. Non-structural masses, as batteries, payload, and engines are fixed during the optimization process and are not used as design variables in the optimization process. Landing system is supposed to be composed by sledges at

Table 2
Technologies assumptions.

Object	**Assumption**
Batt. type	High Eff. LiPo
Batt. energy density	$300 Wh/Kg$
Batt. cycle Eff.	98%
Cell Types	Sunpower Maxeon Cells
Cell Efficiency	23% declared
Brushless Motors Eff.	95% extimated
3 blades props. Eff.	80% extimated

Figure 2. Proposed HALE engines position.

tail junction tip and a carbon leg under the nose (see Ref. [20] for details).

The possibility of taking into account different objectives is one of the most important capability offered by MDO and, for this reason, this modern approach has been chosen. The inclusion of solar energy flux maximization as a specific objective, constitutes the real novelty of the work, since this is not generally involved in a conventional aircraft optimization process. The used MOO procedure has brought to a particular compromise solution in which the characteristic features of the three objectives are evident.

In Sec. 2 some key issues on the concept of Design of Experiment (DOE) for used MDO and MOO approaches are addressed. In Sec. 3 the developed computational environment is described, and in 4 the obtained results are presented and discussed. Finally, some concluding remarks are presented in Sec. 5.

2. Some issues on Design of Experiment for genetic algorithm in MOO

The possibility of taking into account different objectives so finding a best compromise solution, is the most important characteristic of MOO. This powerful capability is improved if one uses tools able to give a wide design space exploration. For this reason, the use of a stochastic method in Multi-Objective Optimization is an appealing solution. Indeed, gradient based method or deterministic methods are very useful if there is a small number of variables or the problem is a single-objective one. Stochastic methods, instead, are typically preferred in the case of high variables number or multi-objective problems. Indeed, they have the very useful characteristic to approach the problem in a global way, Refs. [12, 13]. It is possible to apply genetic algorithm also without knowing explicitly objective function and this makes these algorithms more general for applications.

However, in order to improve robustness and accuracy, in the meanwhile, it is possible to combine a stochastic method with a deterministic one, Refs. [14]. As concerning the optimization algorithm, robustness is the capability of finding the absolute maximum (or minimum) of the objective function. The accuracy, instead, is the capability of going closest as possible to the absolute maximum (or minimum) of the objective function.

In the present work, a MOGA-II method -namely a genetic algorithm- has been used, combined with a gradient based one, Refs. [14]. In this way it is possible to check, at the end of the overall optimization process, the convergence of the solution. Since the gradient based is a local method, it allows to verify other possible better solutions nearby the found one. However, this practice may increase the computational cost, requiring others CPU efforts after the already long calculation time required by the genetic algorithm.

All the genetic based optimization problems need the set-up of the so-called *Design Of Experiment* (DOE). In optimization field DOE can be defined as the space in with are created a first set of individuals or the parents. In order to increase the power of every single technique, it is a good practice to use different method for different optimization process phase. For example, it is possible to start from a Latin Square method for the first analysis, that allows a very good space filling. When a set of feasible designs and Pareto's optima have been found, it is possible to reload them (User Defined DOE) enriching that pool with some random designs or fill the low designs density zones of the space (Incremental space filler).

The definition of the DOE is very relevant and sensitive because a too small DOE could bring to an incomplete exploration of solution. A too wide DOE may imply to a too long and expensive computation. Thus, it is important to have a reasonable dimension of the starting DOE and it is necessary to have a good individuals disposition in the space, without living gaps, for having a wider starting points (parents for a evolutionary method) distribution. Thus, the improvement of the DOE trough the analyses seems to be important by reducing a bit its extension, but without loosing generality, so focusing on a single family of results. There is a strong influence of the DOE in the optimization flow. As the DOE is well defined, as the solution brings to better results. For this reason the design optimization analyses that have been carried out in the present work are not given by single run, but are obtained though different subsequent sub-analyses. For any optimization cycle, the DOE is reloaded and the update of the DOE is composed by chosen designs of the previous one (e.g. Pareto's optima) and other designs. These designs could be added in the design space by using the *incremental space filler* method that allows to fill the gaps in the design space, maximizing the minimum distance from the new point and the old ones, or random generated methods.

The use of a evolutionary method emphasized the DOE relevance more and more. Indeed, the evolutionary method approach has a strong dependency by the first generation members, as the children with the parents. Giving a very pure first generation, the probability of generating a more pure and perfect race is higher. Giving Pareto designs in DOE means to give the elite members of the previous run as parents of the next one. However, an extremely pure parents generation could bring the analysis to a spot result. For this reason when a new DOE is created, some of the best individuals of the previous analysis are loaded, but other, random or not, designs are added too. The melting of different genetic sets enrich and make stronger the population.

3. Model generation tool

A model generation tool for aerostructural analysis has been developed in previous activities - see Refs. [15], [16], [17], [18] and it has been recently renewed and improved by the present one. This tool, called FemWing, is a Fortran executable that is able to generate conventional and unconventional configuration aircraft medium/high fidelity model, starting with a relatively reduced numbers of variables. FemWing also writes input files for structural analyses performed by commercial software and uses the selected solutions. Having the opportunity to generate both structural and aerodynamic models, one has the capability to easily find Pareto solutions. The developed tool is able to model the aircraft structure via Finite Elements analysis and the aerodynamic steady and unsteady load by a panel based approach (namely, Double Lattice Method, Ref. [19]) which avoids the fluid field discretization (typical in Computational Fluid Dynamics). Comparing the render in Figure 1 and the FEM model in Figure 3 it is possible to note a good similarity, so moving the level of fidelity of the used structural modeling. The possibility of direct generation of

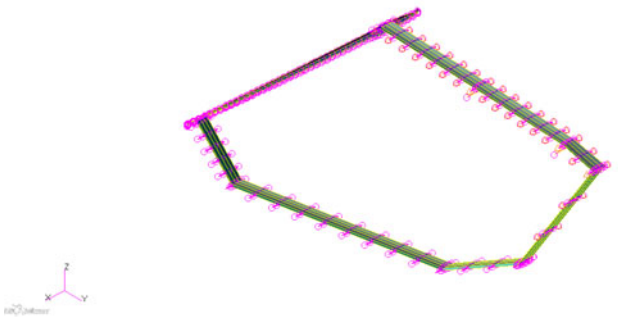

Figure 3. Used HALE FEM.

both structural and aerodynamic models every single iteration allows the possibility to explore an extremely wide range of possible final solutions. FemWing code is now capable of handling closed wing configuration as well. These improvements allowed to carry out optimization analyses on a relevant number of geometries (for further information is possible to see Ref. [20]).

The structural model is generated by using rigid elements, rods and plates elements as available in MSC.NASTRAN® code (see Ref. [21]) . Moreover, it is possible to specify the materials of all the used components and their properties. The flow conditions in terms of flow speed, Mach number and air density (altitude) and panel discretization suitable modeled on the present geometry design are generated by FemWing code as well.

3.1. Proposed HALE FemWing generated model

Since this HALE power source is the electric power coming from the solar panels, the exposed surface improvement is very important. Anyway, a consequent effect to be minimized, it has to be considered the weight increase. Furthermore, in order to have a light but strong (from a structural point of view) aircraft, the design choice has fallen on a closed wing configuration, that allows good aerodynamic performances too. The vertical wing sections closing the structure allow sun rays absorption in case of low-on-the-horizon sun too.

The main characteristics of the proposed initial design HALE are summarized in Table 3. Table 4 (The

Table 3
HALE overall dimensions.

Dimension	Magnitude [m]
Length	15.64
Wingspan	40.0
Height	3.51
Fuselage max. diameter	0.56

data in Table 4 are referred to the HALE half model, as all the optimization results), instead, shows the initial values of three objectives that have been chosen for this MDO:

- Lift-to-drag ratio;
- Sun energy flow;
- Aircraft mass (structural and not structural).

The single-objective optimization of the aircraft mass, typically affects the structural mass, handling geometry and components characteristics (e.g. thickness). Not structural masses are used for modeling as concentrated masses different aircraft components as engines, instruments, avionics and batteries. In the present work a battery consumption model has not been developed, cause the endurance have not be considered as on objective.

The lift-to-drag ratio has been computed as in the following. Lift has ben assumed balancing the aircraft weight (in level flight condition). Given an aspect ratio of $A_R = b^2/S$ the analytic drag coefficient expression is:

$$C_D = C_{D_0} + \frac{{C_L}^2}{\pi A_R e}, \tag{1}$$

where e is the Oswald efficiency number. Then, the lift to drag ratio is:

$$E = \frac{C_L}{C_D}, \tag{2}$$

The three selected objectives are apparently in contrast. The lift-to-drag ratio decrease, increasing the wing surface. Increasing the wing surface could help in sun energy flow enhancement, but does not help in weigh diminution. Thus, the present case makes the optimization as suitable for a Pareto MOO analysis. Some preliminary analyses have been carried out before the optimization started. First of all, two linear static solutions under a gravity load on ground have been carried out (MSC.NASTRAN® solver Sol. 101). The first gravity considered load case is for 1.5g, and the second for 3g. Range of values of g-factor that have been taken into account are compliant to Ref. [6] but excluding the considerations done in this reference on gust load, since the gust occurrence is considered separately in the present analysis (see the end of the present section). The selected gravity loads allow to take into account most of mission stress. Von Mises criterion has been used in order to evaluate possible damages. Furthermore, a 1.5 safety factor has been introduced in the analysis, in accordance with Ref. [6]. Next, a modal analysis has been performed. The results show how such a flexible structure has very low modal frequencies (see Table 5), with consequent potential critical issues on coupling between wing-structure and the engines. Figures 4 shows four significant modal shapes (modes number 3, 5, 7, and 9 respectively). Different aeroelastostatic trim analyses (MSC.NASTRAN® solver Sol. 144) in a range of $U_\infty \in [50m/s - 70m/s]$ have been carried out too. These numerically converged analyses confirmed the longitudinal controllability of the drone. The control surfaces (elevons) are located on middle section of back wing. Moreover, a flutter analysis (MSC.NASTRAN® solver Sol. 145) has been also performed to verify the dynamic aeroelastic stability. The flutter analysis has been carried out in a range of $U_\infty \in [30m/s - 90m/s]$. It is worth to pointing out that the flutter analysis speed range includes the trim analyzed one.

As concerning the gust response analysis, in the present work this has not considering by taking into account a load factor of about 3.8g as done, for example, in Ref. nasa. Indeed, the main scope of this work is to assess a working multidisciplinary optimization environment by analyzing an unconventional HALE configuration in its operating condition at its loitering altitude, so assuming that turbulences at these altitudes are rarely present (see Ref. [22]). However, aeroelastic gust response analyses (via Nastran solver Sol 146, Ref. [21]) on the initial and final configurations were carried out. The obtained results (see Ref. [20]) gave a maximum value for load factor up to 3.25 (after including also a safety factor of 1.5).

Table 4
Design starting point.

Lift-to-drag ratio	**Energy flow [W]**	**Mass [kg]**
21.4	8177.7	421.0

Table 5
Natural frequencies list.

Mode	**Frequency [Hz]**
Mode 1	0.87
Mode 2	1.85
Mode 3	1.98
Mode 4	2.72
Mode 5	2.81
Mode 6	4.29
Mode 7	4.86
Mode 8	5.69
Mode 9	6.44
Mode 10	7.18
Mode 11	7.44
Mode 12	9.35
Mode 13	9.94
Mode 14	16.00
Mode 15	16.28
Mode 16	16.71
Mode 17	17.09

3.2. Optimization flow

The optimization has been carried out by considering the following items:

- V_∞ is assumed constant. This assumption has been taken because of the HASP typical missions. The RPAS, used as a pseudo satellite, needs to fly with a constant cruise speed, as a satellite does.
- It is necessary to point out as the weight of the aircraft changes every optimization iteration.
- For every optimization iteration the aircraft has been assumed flying in trimmed condition, with a specific α_{Trim}, that allows to define the lift force as $L = W$. Furthermore, this class of UAVs does not perform particular maneuver, that makes this assumption more reasonable.
- Basing on what has been just said, the the L/D ratio that has been included as an objective of the optimization problem is not intended to be linked to the minimization of the necessary

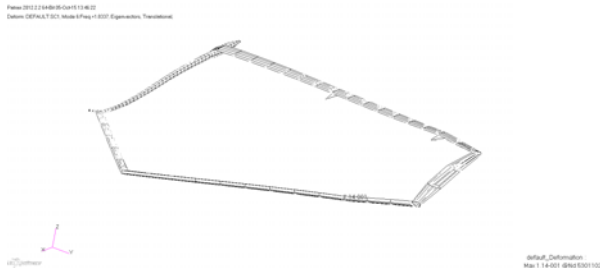

(a) *Mode # 3*

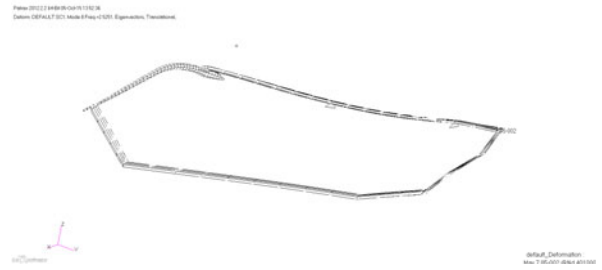

(b) *Mode # 5*

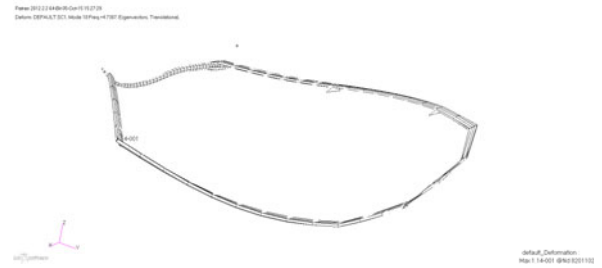

(c) *Mode # 7*

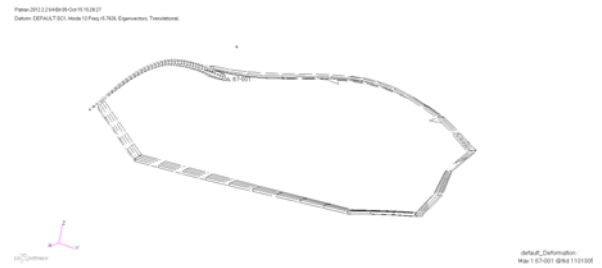

(d) *Mode # 9*

Figure 4. Four significant modal shapes.

power, but is the $L/D@\alpha_{Trim}$. The present work selected the L/D ratio as the capability of the aircraft of carrying a large payload, for a long time, over a long distance. The minimization of the necessary power could be analyzed at a later time.

Figure 5 shows the used optimization flow. Also if in these application is common practice to use surrogate model procedure, Ref. [23], the use of the presented optimization approach (genetic algorithm) guarantees that every generated result is unique, as the child from the parents. While presenting similar features to parents, it is completely different. This allows you to get results that at the beginning of the calculation were not even predicted.

For performing the optimization two different commercial software have been used. The first one is modeFRONTIER® . It is a Process Integration Design Optimization (PIDO) software that allows the work flow management of all the optimization necessary entities, Ref. [24]. The second one is MSC.NASTRAN® , a Computational Structural Mechanic (CSM) software which collects a suite of structural and aeroelastic solvers, Ref. [21].

It could be useful to distinguish between two different type of used variables in the optimization process:

- *design variables*: This class of variables is the one that the optimization software is able to modify every single iteration in a user specified range;

- *fixed parameters*: Parameters that, once fixed in the preliminary phase, cannot be modified automatically by the optimization tool.

After reading the input files, the model generation tool (FemWing) starts creating the structural model and the aerodynamic DLM (Doublet Lattice Method) discretization (Ref. [19]). The conditions for sing a DLM lifting surface approach is linearized flow (compressible and unsteady) with undisturbed flows assumed to be uniform.

The following analyses are performed during the optimization process (see Fig. 5). First, a linearly static analysis in which the drone is loaded as undergone on ground to its own weight only. A second linear static analysis in which the UAV is loaded with three times its own weight (see comments on the previous subsection). Since HALEs typically land with very smooth trajectories and with final approach perfectly aligned to the ground, limiting the choice of load factor up to 3 seemed to be a reasonable choice. Indeed, there is not a touchdown on the back landing system. In Ref. [6] a value of 1.5 was recommended for taking into account taxing bump stresses. Indeed, a higher load factor up to 3.8 as recommended in Ref. [6], should take into account also the occurrence of gust. However, this value was not assumed for stress evaluation in the present work (see also comments in previous section) since the gust response analysis was performed only *a priori* and *a posteriori* of the optimization process so allowing more possibility for final design solutions. However, future works would include the analyses of different flight phases like, for example, the low altitude flight with related aeroelastic gust analysis included in the optimization loop.

Finally, aeroelastostatic trim analyses are included in the optimization loop. As commented in the previ-

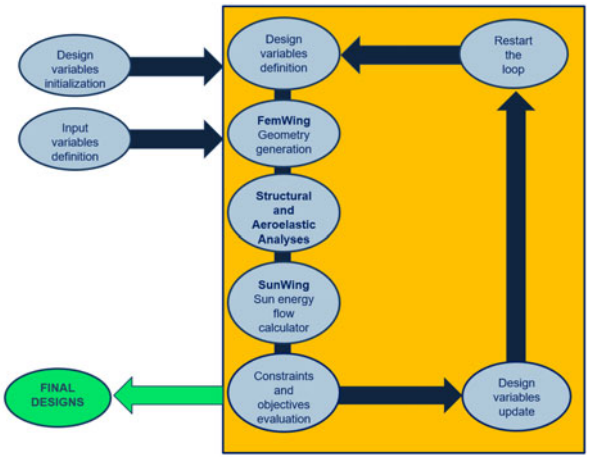

Figure 5. Optimization flow chart.

ous subsection, the longitudinal flight stability of the obtained model is ensured by the fact that obtained trimmed solution is numerically and physically stable.

After this first analyses call, the Sun energy flow (trough the solar panels) estimator, denoted as **SunWing**, is launched (see Fig. 5). **SunWing** is a "in-house" tool that, once read the geometry of the wing and tail sections, it is able to compute the global sun energy flow (ϕ_{Tot}) through the solar panels as illustrated in the following. This operation is carried out without taking into account the trajectory of the aircraft, but only the sun position during the day. This because the UAV moves with plain circular trajectories without rolling or performing others evolution that could seriously varying the relative angle between the sun rays incidence and the solar panels surface normal. The flow estimation has been performed in the following way:

$$\phi_{Tot} = \int_{S_{Tot}} \vec{v}_{sun} \cdot \vec{n} dS \simeq \sum_{i=1}^{N_{wing_{sections}}} S_i \vec{n_i} \cdot \vec{v}_{sun} + \sum_{j=1}^{N_{tail_{sections}}} S_j \vec{n_j} \cdot \vec{v}_{sun} \quad (3)$$

where $\vec{v}_{sun}$ is the sun rays energy vector and $\vec{n}_i$ the normal to the surface of the i-th panel. S_i is the surface area of the n^{th} panel of the wing surface.

Using a half model it is sufficient to take into account only half day, then, the morning until midday, assuming also the previous considerations about the trajectory. Assuming that the sun sets at 6:00 AM, if the Azimuth occurs at 12:00, it is possible to divide the Sun climb in different steps. For each steps one can estimate a direction of $\vec{v}_{sun}$ with respect to $\vec{n}$ of local panel. Using this information, it is possible to compute the energy flow (here ϕ_{Sun}) that runs over the cells. Inserting this objective in the MOO loop is an original issue presented in this work.

After this information, it is possible to define constraints and objectives. The set constraints are defined as limit for the stresses of the structure (different for Aluminum skeleton and Carbon skin) and for the trim angles which values are computed by MSC.NASTRAN® in the trim solution (MSC.NASTRAN® solver Sol. 144), called during each optimization loop. The limit values (see Tab. 6) are set in modeFRONTIER® that checks (every loop) possible out of boundaries results. Limits on stresses have been defined basing on materials properties. Yielding stress has been used for Aluminum (here 2024-T3 Aluminum alloy). Ultimate stress has been used for composite skin (carbon fibers fabric). The high degree of nonlinearity typical of these configurations makes the use of reduced order models extremely difficult. The linear approach, as the one used in this work, is suitable for preliminary design. For this reason the buckling analysis have been performed in linear field and did not put evidence criticality on the studied HALE, but only higher order or more detailed nonlinear analyses should be used to avoid large modeling errors (see Ref. [25]). Control surfaces deflection for these planes are very high, but increasing the elevator excursion, the lift to drag ratio decreases.

Finally, it is necessary to update the used design variables presented in Tab. 7. All the variables are updated varying them in a selected range. For each variable the variation range, the delta value and the starting value have been defined.

4. Results

As preliminary analyses of the multi-objective optimization, three different Single Objective Optimization (SOO) have been carried out. In this way it is possible to estimate the *Nadir* and the *Utopia* points

Table 6
Constraints in the analyses.

Constraint	Description	Min.	Max.
STRESS (Von Mises)	CONROD traction (Aluminum structure)	0 MPa	360MPa
	CONROD compression (Aluminum structure)	-360MPa	0MPa
	CQUAD4 (composite skin)	0MPa	350MPa
Constraint	**Description**	**Abs. Min.**	**Abs. Max.**
TRIM ANGLES	Angle of attack	0°	10°
	Elevator angle	0°	10°

in the space of objectives. Indeed, the *Utopia* point (see Tab. 8) is the point whose coordinates in the objectives space are the three best value obtained from the SOO analyses. It is used for scaling all the results in the subsequent MOO analysis. The stop criterion used for all the analyses has been the continuous monitoring of the history charts. When the history charts have reached the *plateau* the analysis has been stopped. It seemed to be a good compromise between results validity and computation time. *Nadir* (see Tab. 9) point is the same but with the worst values. In the following sections plots, the result have been normalized with respect to the *Utopia* point. For this reason, plot reported values are not-dimensional.

4.1. SOO analyses results

In order to show the results of the three single objective analyses, the history charts and the statistic distribution of the selected designs are shown in Fig. 6. A result is defined as "feasible" if it satisfies the constraints, unfeasible when it does not. A design is classified as "error" if some problem occurred in model generation or the analyses cannot be performed. About the computational efforts, the three analyses, launched in parallel, asked a computational time between $11h$ and $13m$ on 64gb of RAM, i7-4930K CPU 3.40GHz, running Windows 10 ®64-bit machine.

As it is possible to see, the reduced number of errors (Fig. 7) means that high level modeling skills seem to be reached, also if the configurations are really unconventional. The modeling fidelity ensures good level in the analysis too. A considerable portions of the pie charts are filled by unfeasible designs (Fig. 7). This means that the analyses have well covered the design space, often impacting the constraints. Furthermore, the main reason of the un-feasibility, is related to the trim. It was expected because the vehicle trimming is performed at a very low value of the air density ($0.08Kg/m^3$ at $20Km$ of altitude). However, it is possible to see that the higher percentile of designs is classified as feasible. Having a lot of feasible design means good improvements and further generations higher quality.

The isometric views of the aircraft after the SOO analyses are presented in Figs. 8, 9, and 10. Their

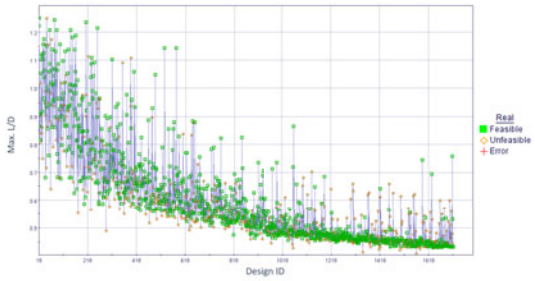

(a) *Max. L/D history chart.*

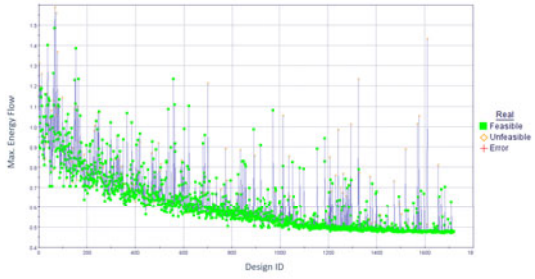

(b) *Max. energy flow history chart.*

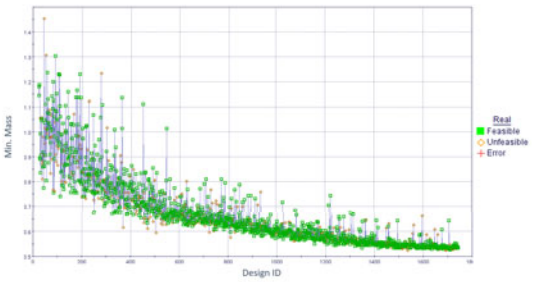

(c) *Min. Mass history chart.*

Figure 6. Single Objective Optimization (SOO) history charts.

final geometrical dimension and objectives in comparison to the presented starting point are showed in Tables 10, 11, 12. It is possible to realize how the three objective are in contrast one each other. In par-

Table 7
Design variables that modeFRONTIER® can modify during the optimization loop.

Design variables	**Variation range**	**Δ value**	**Starting value**
	WING		
Root skin thick	[0.0005;0.0015]	0.0005	0.0010m
Web thick	[0.0015;0.0085]	0.0035	0.0050m
Root spar area	[6E-06;10E-06]	4E-06	8.0000E-06m^2
Root stringer area	[3E-06;7E-06]	4E-06	5.0000E-06 m^2
Chords	[0.500;2.500]	1.0	1.50 m
Span_1	[7.60;9.60]	1.0	8.60 m
Span_2	[7.10;9.10]	1.0	8.10 m
Span_3	[1.88;3.88]	1.0	2.88 m
Span_4	[5.34;7.34]	1.0	6.34 m
Sweep_1	[2.52;12.52]	5.0	7.52°
Sweep_2	[3.08;13.08]	5.0	8.08°
Sweep_3	[6.581;16.581]	5.0	11.581°
Sweep_4	[-61.58;-51.58]	5.0	-56.58°
Dihedral_1	[1.01;11.01]	5.0	6.01°
Dihedral_2	[1.01;11.01]	5.0	6.01°
Dihedral_3	[-5.0;5.0]	5.0	0.0°
	TAIL		
Root skin thick	[0.0005;0.0015]	0.0005	0.0010m
Web thick	[0.0015;0.0085]	0.0035	0.0050m
Root spar area	[6E-06;10E-06]	4E-06	8.0000E-06m^2
Root stringer area	[3E-06;7E-06]	4E-06	5.0000E-06 m^2
Chords	[0.500;2.500]	1.0	1.50 m
Span_1	[1.70;3.70]	1.0	2.70 m
Span_2	[12.93;14.93]	1.0	13.93 m
Span_3	[1.94;3.94]	1.0	2.94 m
Sweep_1	[-5.0;5.0]	5.0	0.0°
Sweep_2	[-14.11;-4.11]	5.0	-9.11°
Sweep_3	[-49.476;-39.476]	5.0	-44.476°
Dihedral_1	[-49.372;-39.372]	5.0	-44.372°
Dihedral_2	[-3.00;7.00]	5.0	2.00°
Dihedral_3	[4.6;14.6]	5.0	9.6°
	FUSELAGE		
Skin thick	[0.0005;0.0015]	0.0005	0.0010m
Stringer area	[3E-06;7E-06]	4E-06	5.0000E-06 m^2

Table 8
Utopia point coordinates.

Lift-to-drag ratio	ϕ_{Sun}**[W]**	**W [Kg]**
49.6	17364.235	222.0

Table 9
Nadir point coordinates.

Lift-to-drag ratio	ϕ_{Sun}**[W]**	**W [Kg]**
15.0	3272.51	735.0

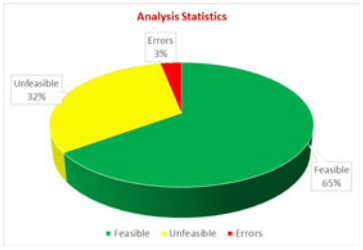

(a) *Statistic designs distribution for max L/D.*

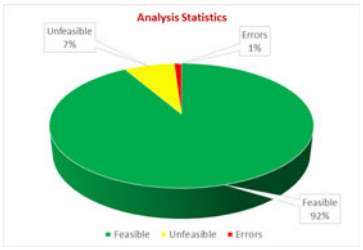

(b) *Statistic designs distribution for max energy flow.*

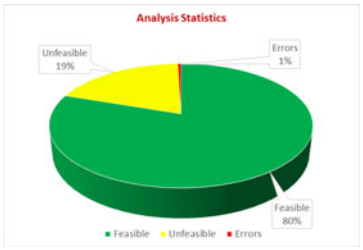

(c) *Statistic designs distribution for min. mass.*

Figure 7. SOO analyses statistics.

ticular, it is possible to see how, in order to decrease the L/D ratio (Tab. 10), the optimization process try to reduce the dimension of the front wing and, consequently, the increasing of the wingspan means an increasing of the mass. Moreover, the optimization of the absorbed sun power pass through the increasing of the surfaces (Tab. 11). For this reason the maximum

(a) *Isometric view.*

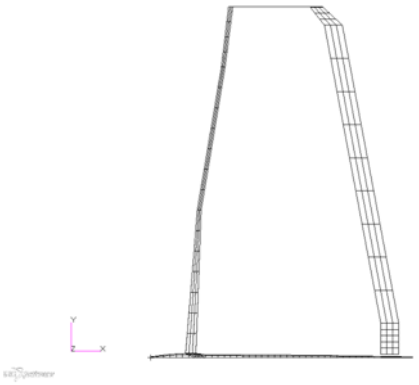

(b) *Top view.*

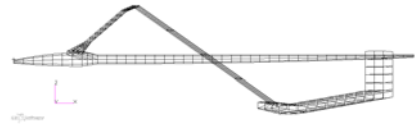

(c) *Side view.*

(d) *Front view.*

Figure 8. Maximum L/D design.

Table 10
Max. L/D analysis model information and objectives values.

Dimension	**Magnitude**
Lenght	15.64$[m]$
Wingspan	44.2$[m]$
Height	4.44$[m]$
Fuselage max. diameter	0.56$[m]$
Wing Loading	77.82$[N/m^2]$

L/D	ϕ_{Sun}**[W]**	**Mass [Kg]**
49.6(+79.4%)	9115.88(+10.5%)	565.0(+29.2%)

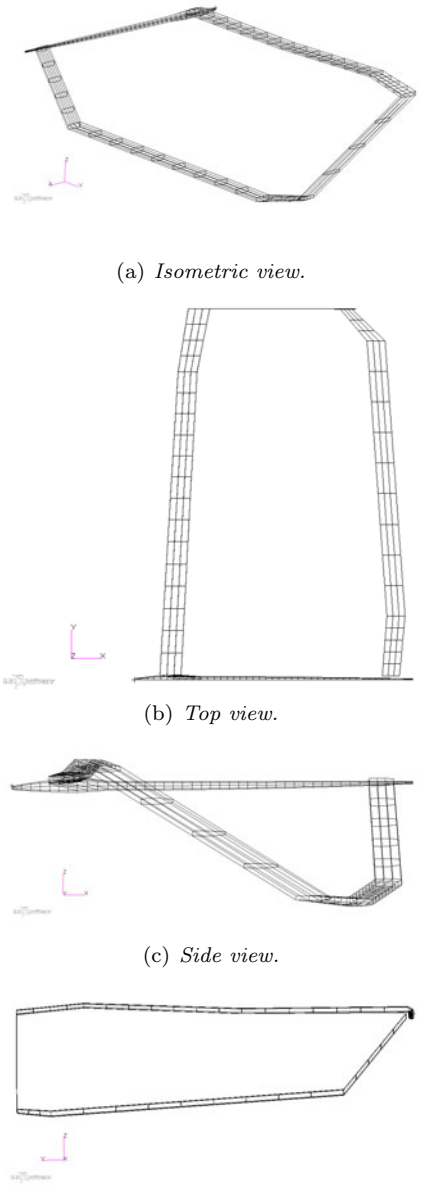

(a) *Isometric view.*

(b) *Top view.*

(c) *Side view.*

(d) *Front view.*

Figure 9. Maximum power-flow design.

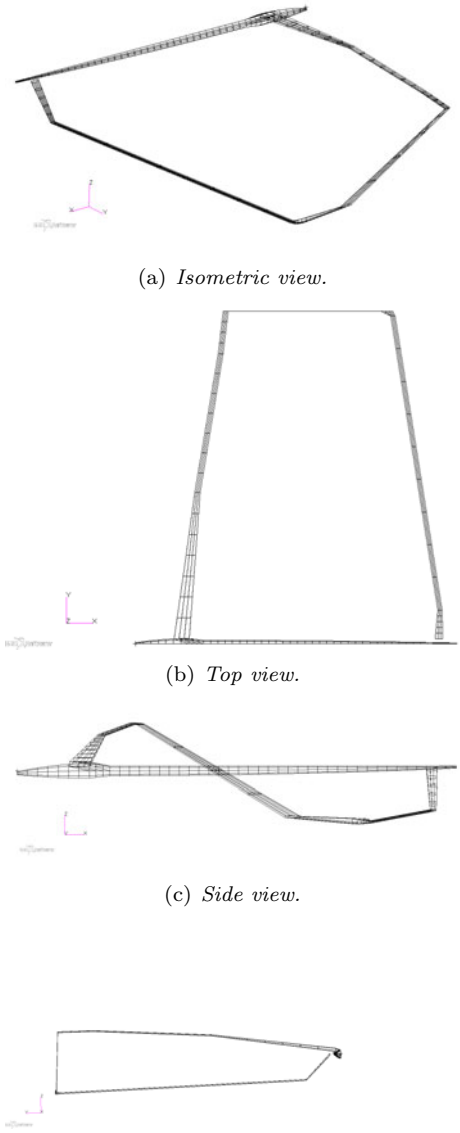

(a) *Isometric view.*

(b) *Top view.*

(c) *Side view.*

(d) *Front view.*

Figure 10. Minimum mass design.

energy flow design in Fig. 9 is characterized by higher values of chords length. This is in opposition to the reduction of the aerodynamic drag and the decreasing of the mass. This model wingspan is still higher than the previous one and the HALE is taller too so increasing the absorbed power when the sun is low on the horizon, thanks to the very extended vertical section.

In order to reduce the mass, the wing and tail dimensions are reduced to the minimum. The wingspan is reduced and, looking at the front view, the entire model seems to be smaller than the others (see Fig. 10 and Tab. 12). Note that all these results correspond to utopia designs. Note also that the high increments of the three objectives are possible only because the three objectives are not considered all together.

4.2. MOO analysis result and best compromise model

After the three SOO analyses, the MOO analysis has been performed as well. In Figure 11 it is possible to see the three history charts of the analysis (the computation time about $98h$, on a computer with a 64Gb of RAM and with i7-4930K CPU computer). Using a genetic algorithm approach, it is possible to see the presence of the floating, but also a good convergence

Table 11
Max.energy flow analysis model information and objectives values.

Dimension	**Magnitude**
Lenght	$15.64[m]$
Wingspan	$45.2[m]$
Height	$5.91[m]$
Fuselage max. diameter	$0.56[m]$
Wing Loading	$52.71[N/m^2]$

L/D	ϕ_{Sun}**[W]**	**Mass [Kg]**
15.0(-43%)	**17364.235**(+71.93)	735.0(+51.32)

Table 12
Min. mass analysis model information and objectives values.

Dimension	**Magnitude**
Lenght	$15.64[m]$
Wingspan	$35.2[m]$
Height	$3.9[m]$
Fuselage max. diameter	$0.56[m]$
Wing Loading	$78,01[N/m^2]$

L/D	ϕ_{Sun}**[W]**	**Mass [Kg]**
24.5(+14%)	3362.12(-83.5%)	**222.0**(-61.9%)

slope is achieved (Fig. 11). One of the most important results is the very reduced number of errors (Fig. 13). The relevance of this result is linked to the very high capability in managing very unconventional geometries in an unconventional optimization loop. The peculiarity of this optimization loop, indeed, is connected to the decision of inserting the energy flow as an objective. The reduced number of errors also proves the capability of cooperation of the developed software (FemWing and SunWing) and the commercial ones like modeFRONTIER®, the PIDO (Process Integration and Design Optimization) software, and MSC.NASTRAN® CSM solver. The unfeasible designs number decreased, going through the designs generation. The value reported in Fig. 13 is an overall value that takes into account the generated unfeasible designs with respect to the total designs number.

The final solution given by the model in Fig.14 has been chosen in the Pareto surface in objectives space depicted in Fig. 12, after evaluating the design point having the minimum distance d_{min} to the utopia point. Namely, this distance to be minimized is defined in the objective space as:

$$d_{min} = \sqrt{\left(\frac{E - E_{ut}}{E_{ut}}\right)^2 + \left(\frac{\phi - \phi_{ut}}{\phi_{ut}}\right)^2 + \left(\frac{M - M_{ut}}{M_{ut}}\right)^2} \tag{4}$$

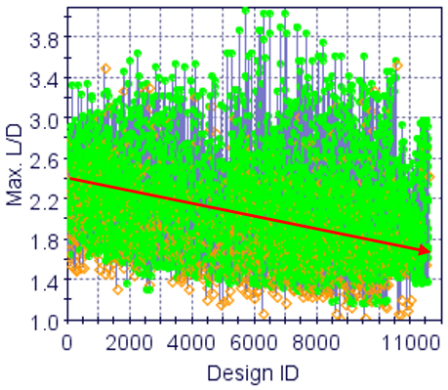

(a) *Maximum L/D history chart.*

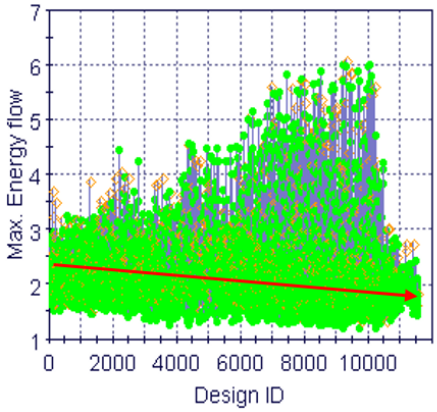

(b) *Maximum energy flow history chart.*

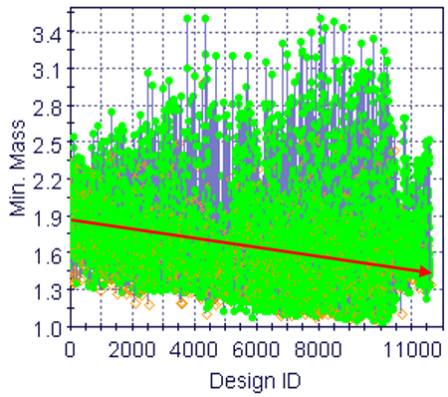

(c) *Minimum Mass history chart.*

Figure 11. MOO history charts.

Then, it is possible to obtain the parametric plot of the Pareto's front with the distance from the utopia point, as shown in Fig. 15. In Figure 15 one can see the point colors changing from yellow to magenta. The utopia point is the red one (in the origin). It is possible to see how the Pareto's optimal design points

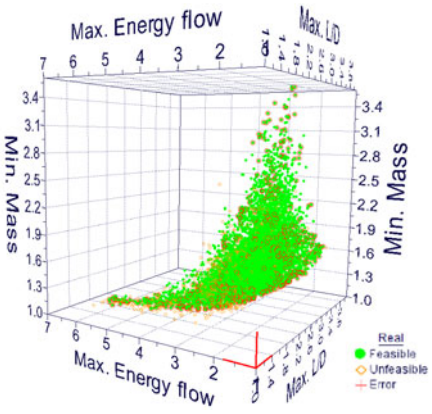

Figure 12. Pareto front.

(a) *Statistic designs distribution.*

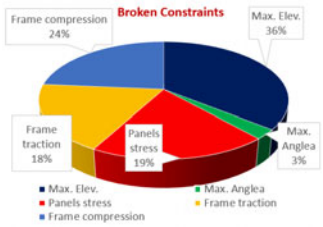

(b) *Constraints summary.*

Figure 13. MOO analyses statistics.

(a) *Isometric view.*

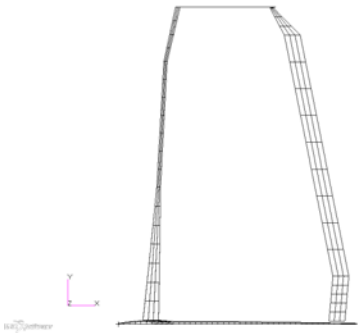

(b) *Top view.*

(c) *Side view.*

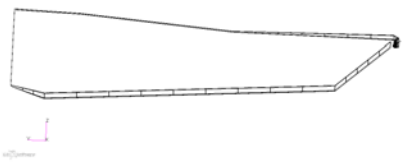

(d) *front view.*

Figure 14. MOO best compromise model.

are more concentrated in the minimum distance zone. It is interesting to see the small difference between the utopia point given by the three single objective analyses, and the one given by the MOO analysis.

Comparing the two sets of components of the utopia point (L/D ratio, energy flow, mass) for the SOO and MOO analyses, one has:

$$\Delta_{ut} = |\mathbf{X}_{ut\ SOO} - \mathbf{X}_{ut\ MOO}| = [14.7\%, 19.3\%, 3.1\%]\,,$$

Indeed, it is possible to see how the single objective analyses guess it is not so far from the one found out with the MOO, as it is possible to see in Fig. 15.

The capability of MOO is the possibility to find out a final model that tries to optimize all the objectives, so describing the compromise between them. For this reason, looking at the increments of Tabs. 10, 11, 12 and comparing them with the ones in Tab. 13, one could see that the objectives improvements are smaller than the SOO obtained ones. In Fig. 14, the reached

Table 13
MOO best compromise model informations.

L/D	$\boldsymbol{\phi_{Sun}}$**[W]**	**W [Kg]**
31.0 (+37%)	10015.27 (+20%)	373.0 (-12%)

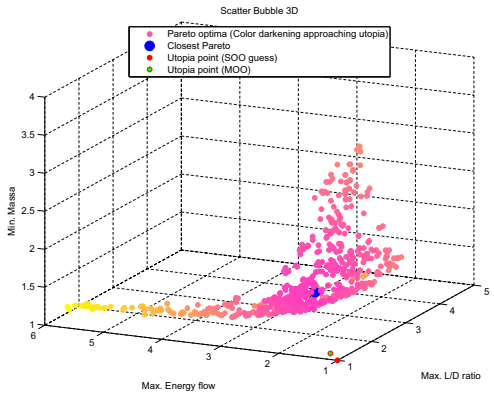

Figure 15. Pareto front parametrized with the distance from the utopia point.

compromise in the optimized configuration is shown. In order to reduce the drag, for improving the L/D ratio, the front wing extension seems to be smaller than the tail one. The tail, instead, has a higher surface, for increasing the caught sun power. This confirms that the two objectives are in opposition. The minimization of the mass is helped by the reduction of the structures, moving in opposition to the improvement of the caught sun power. The estimated absorbed power is consistent with the value presented in Ref. [26]. Table 14 shows the MOO best compromise Pareto design model information. A very good results has been found for

Table 14
MOO best compromise model informations.

Dimension	**Magnitude**
Lenght	$15.64[m]$
Wingspan	$60.42[m]$
Height	$4.97[m]$
Fuselage max. diameter	$0.56[m]$
Wing Loading	$47,25[N/m^2]$

the lift to drag ratio. This result has been compared with the best lift to drag ratio available for this configuration, analytically found through the aerodynamic polar equation (Ref. [27]). Substituting (1) in (2), is possible to find out the maximum lift coefficient that gives the maximum lift to drag ratio. A maximum value for E_{max} equal to 32.77 has been obtained. As it is possible to see, the result of the optimization is very close to the maximum lift to drag ratio possible for this model. The difference is only of a 5.5%. It is a very important result, because this shows how, the best compromise result is really the best that it is possible to find out for the present model.

4.3. Other examples of determined Pareto design points

In order to have a simple comparison, other two Pareto design points are shown. The first one is located on the right of the closest to utopia point (here RCU Fig. 16), the second on the left (here LCU Fig. 16). The

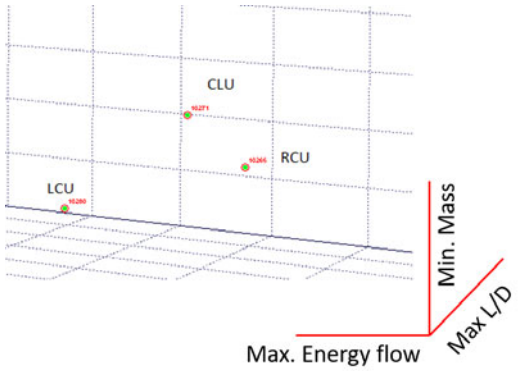

Figure 16. Optimal designs in objectives space.

two Pareto design points results are given in Tab. 15. For the RCU is possible to observe how the MOGA

Table 15
LCU and RCU Pareto design points objectives value.

Lift-to-drag ratio	ϕ_{Wing}**[W]**	**W [Kg]**
	RCU	
25.4	10305.93	336.0
	LCU	
31.8	7462.60	318.0

had a preference for weight and energy flow, giving a lower lift to drag ratio. About LCU, it is possible to see how the optimization code emphasizes the improvement of mass and lift to drag ratio rather than the energy flow that is almost half from the previous case. The other important characteristic that it is necessary to point out is that the constraints are more stressed than RCU. The finite elements models of RCU and LCU are shown in Fig. 17. The geometries are so similar in shape, but LCU model is a bit smaller (see Tab. 16). Concluding, the comparison of the new points with the closest to utopia design shows

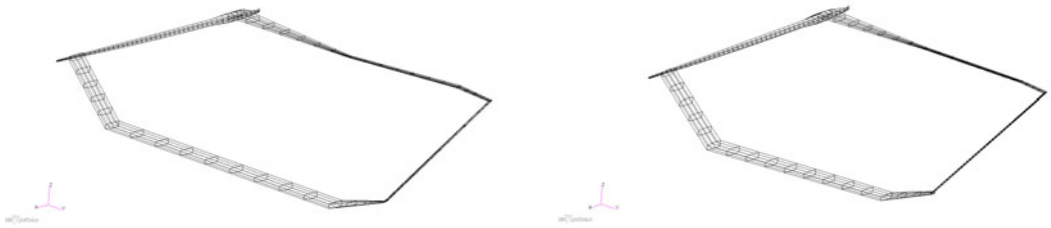

(a) *RCU.* (b) *LCU.*

Figure 17. RCU and LCU finite elements models.

Table 16
LCU and RCU models dimensions.

Dimension	**LCU Magnitude [m]**	**RCU Magnitude [m]**
Lenght	15.64	15.64
Wingspan	33.20	44.40
Height	3.52	5.05
Fuselage max. diameter	0.56	0.56

how the first shown solution is really the best compromise result. If one moves in any direction from this solution, the results turn in direction of one or another objective.

5. Concluding remarks

MDO and MOO approaches are used in the present paper for the preliminary design of an unconventional HALE configuration for a HAPS, so involving the cooperation of different engineering branches (structures, aerodynamics, propulsion systems and power, flight dynamics). More specifically, a joined-wing configuration for the HAPS design – namely, Box Wing System or Prandtl's wing – has been optimized.

SOO analyses have been performed by considering three different separated objectives (lift to drag ratio increasing, mass minimization and caught solar energy maximization) and the obtained design solutions revealed to be in contrast each other.

Therefore, the needs of considering power systems in the optimization process – which is an unusual issue applied to an aeronautical MOO problem – has brought to the development of a dedicated algorithm. The capability to have an updated model generated for every single design iteration, has been applied to an unconventional Prandtl wing system HAPS. Since the developed model generator is able to provide reliable FE models with a good level of robustness, the applied genetic algorithms revealed faster on providing the optimized solutions.

The obtained Pareto solutions resulted to be the best compromise designs. As it has been verified, the lift to drag ratio takes the best value as possible for the actual configuration. The Pareto nature of the obtained solutions is clearly shown by the fact that the maximization of the solar-panel covering surfaces (useful to maximize the absorbed power) is in contrast with the HAPS weight decrease and with the minimization of the aerodynamic drag too. The locus represented by all the design each-contrasting solutions at limit of the above compromises –namely, the Pareto surfaces – is determined. Finally, a best solution among the Pareto available ones has been selected by minimizing the distance between the Pareto surface points and the Utopia point. The present work is limited to optimize a single mission phase or segment. Future development will take into account other mission phase -as takeoff, landing, ascent (considering turbulence)- and other design aspect -as power absorption model- to be included in optimization loop.

Acknowledgements

This work has been supported by Sapienza, Bandi Ricerca 2017.

REFERENCES

1. Zephyr, the High Altitude Pseudo-Satellite, AIRBUS Defense and Space, HTTP://DEFENCE.AIRBUS.COM/PORTFOLIO/UAV/ZEPHYR.
2. G. Romeo, G. Frulla, and E. Cestino, *Design of a high-altitude long-endurance solar-powered unmanned air vehicle for multi-payload and opera-*

tions, J. of Aerospace Engineering, Proc. IMechE Vol. 221 Part G, September 2006
3. NASA, *NASA Armstrong Fact Sheet: Helios Prototype*, https://www.nasa.gov/centers/armstrong/news/FactSheets/FS-068-DFRC.html.
4. Facebook Inc., *Aquila drone*, https://www.youtube.com/watch?v=NzLkmcduYuc.
5. Solar Impulse SA 2016, *Solar Impulse*, http://www.solarimpulse.com/.
6. Hall D. W., Hall S. A., *Structural sizing of a solar powered aircraft*, NASA Contractor Report 172313.
7. Prandtl L., *Induced drag of multiplanes*, Technische Berichte, Volume III, No. 7, March 1924.
8. Frediani, A., *The Prandtl Wing. Lecture series: Innovative Configurations and Advanced Concepts for Future Civil Transport Aircraft*, ISBN 2-930389-62-1, Von Karman Institute, VKI 2005-06, 2005.
9. Werner-Westphal C., Heinze W., Horst P., *Multidisciplinary Integrated Preliminary Design Applied to Unconventional Aircraft Configuration*, Journal of Aircraft, Vol. 45, No. 2, 2008.
10. Willcox, K.,*Collaborating for multi-disciplinary design*, Aerospace America-Year in Review, No. 12, Reston, Virginia (US), 2015.
11. Torenbeek, E.,*Advanced Aircraft Design: Conceptual Design, Analysis and Optimization of Subsonic Civil Airplanes*, John Wiley & Sons, Ltd., West Sussex, United Kingdom, 2013.
12. Arora,J. S.,*Introduction to Optimum Design*, McGraw-Hill International Edition-Mechanical Engineering Series, Singapore, 1989.
13. Haftka R. T., Gürdal Z.,*Elements of structural optimization, third Revised and Expanded Edition*,Kluwer Academic Publishers, 1993.
14. Rigoni E.,Poles, S., *NBI and MOGA-II, two complementary algorithms for Multi-Objective optimizations*,Pratical approach to Multi-objective Optimization, Dagstuhl Semina Proceedings, Vol. 4461, Wadern, Merzig-Wadern, Saarland, 2005.
15. Mastroddi, F., Gemma, S., *Analysis of Pareto Frontiers for Multidisciplinary Design Optimization of Aircraft*, Aerospace Science and Technology, Vol. 28, pp. 40-55, 2013, DOI 10.1016/j.ast.2012.10.003, 2012.
16. Gemma, S., Mastroddi, F., *Nonlinear modelling for Multi-Disciplinary and Multi-Objective Optimization of a complete aircraft*, Aerotecnica Missili e Spazio, Journal of Aerospace Science, Technologies & Systems, Vol. 92, No. 1-2, March-June 2013, pp. 61-68.
17. Gemma, S., Mastroddi, F., *Genetic and Graient-Based Algorithms for the Multi-Objective Optimization of Aircraft Design with Aeroelastic Constraints*, International Forum on Aeroelasticity and Structural Dynamics, Paper IFASD-2015-075, Saint Petersburg, Russia, June 28 - July 2, 2015.
18. Gemma, S., Mastroddi, F., *Multi-Disciplinary and Multi-Objective Optimization of an Unconventional Aircraft Concept*, AIAA 2015-2327, 16-th AIAA/ISSMO Multidisciplinary Analysis and Optimization Conference, 22-26 June 2015, Dallas, TX. eISBN: 978-1-62410-368-1, DOI: 10.2514/MMAO15.
19. Rodden W. P., Taylor P. F., McIntosh S. C. Jr., *Improvements to the Doublet–Lattice Method in MSC.NASTRAN*.
20. Travaglini, L. M., *Multi-objective optimization for the design of a High-Altitude Long-Endurance unmanned vehicle*, Master thesis in aeronautical engineering, Sapienza Università di Roma, Roma, 2016.
21. MSC Software GmbH, *MSC.Nastran Quick Reference Guide*, 2012.
22. Steiner, R., *A review of NASA high-altitude clear air turbulence sampling programs*, Journal of Aircraft, Vol. 3, No. 1 (1966), pp. 48-52.
23. Deng, H., Yu, X., Yin, H., Deng, F. *Trim drag prediction for blended-wing-body UAV configuration.*, Transactions of Nanjing University of Aeronautics and Astronautics, 32 (1), pp. 133-136, 2015.
24. ESTECO s.r.l., *modeFRONTIER 3.1 User Manual*,http://www.esteco.com/home/mode_frontier/mode_frontier.html.
25. Demasi L., Cavallaro R., Razón A. M., *Postcritical Analysis of PrandtlPlane Joined-Wing Configurations*, San Diego State University, San Diego, California 92182.
26. Youngblood J.W., Talay T.A., Pegg R.J., *Design of Long-Endurance Unmanned Airplanes Incorporating Solar and Fuel Cell Propulsion*, NASA Langley Research Center, Hampton, Virginia.
27. Anderson J. D., Jr., *Fundamentals of Aerodynamics*, Third Edition, McGraw-Hill Education, New York City, New York, 2001.
28. Cipolla V., Frediani A., *Design of Solar Powered Unmanned Biplanes for HALE Missions*, Springer, 2012.
29. Romeo, G., Frulla, G., Cestino, E., *Design of a High-Altitude Long-Endurance Solar-Powered Unmanned Air Vehicle for Multi-Payload and Operations*, Proceedings of the Institution of Mechanical Engineers, Part G: Journal of Aerospace Engineering. Vol 221, Issue 2, pp. 199 - 216. 2007
30. Noll et al., *Investigation of the Helios Prototype Aircraft Mishap*, NASA 2004
31. Cipolla, V., *Design of solar powered high altitude long endurance unmanned biplanes*, PhD thesis, University of Pisa, Ph.D. Course in Aerospace Engineering (2010)